Correlation-Based Polarization Demultiplexing for Clock Recovery in Coherent Optical Receivers

Valery N. Rozental[1], Bill Corcoran[1,2] and Arthur J. Lowery[1,2]

[1]*Dept. of Electrical & Computer Systems Engineering, Monash University, Clayton, VIC, 3800, Australia*
[2]*Centre for Ultrahigh-bandwidth Devices for Optical Systems (CUDOS), Australia*
valery.rozental@monash.edu

Abstract: We propose and experimentally validate a novel method for polarization demultiplexing, based on intensity sample cross-correlation of polarization-multiplexed signals. The method allows to avoid PMD-induced failure conditions in digital clock recovery with limited computational complexity.

OCIS codes: 060.0060 Fiber optics and optical communications, 060.1660 Coherent communications.

1. Introduction

Polarization-diversity coherent optical receivers seamlessly separate the polarization-multiplexed (PM) signals by digitally aligning the state-of-polarization (SoP) of the incoming signal with that of the local oscillator (LO) using a multiple-input, multiple-output (MIMO) dynamic equalizer (DE). Nevertheless, polarization alignment prior to dynamic equalization is attractive for several reasons. For example, it ensures correct operation of clock recovery algorithms by avoiding combinations of SoP and differential group delay (DGD) that result in clock information loss [1,2]; it can increase DE convergence speed and robustness against singularities (situations where both MIMO outputs converge to the same source) of non-data-aided algorithms [3–5].

Several polarization demultiplexing (PolDemux) algorithms have been proposed in the literature. Szafraniec *et al.* used Stokes space transformation, inferring the polarization state by plane fitting within the Poincaré sphere [3]. Muga and Pinto overcame the fitting complexity using adaptive tracking [4]. Building up on the Stokes space approach, Ng *et al.* used extended Kalman filter-based SoP tracking for clock tone enhancement [1]. Stojanović *et al.* [2], and Sun and Wu [6], used the clock tone strength as the cost function to adaptively find the SoP defining angles. Finally, Schmogrow *et al.* used intensity fluctuations to extract SoP information [5].

In this work we propose an alternative approach; extracting the SoP information from the intensity cross-correlation (ICC) between the polarization-multiplexed signals. The ICC can be efficiently implemented via FFT, whose computational complexity is halved, because intensity is real-valued [7]. Experimental validation shows successful clock tone recovery for a Nyquist 32-GBd PM-16QAM signal with DGD of half the symbol period, and 45° SoP rotation.

2. Correlation-based Polarization Demultiplexing

To illustrate the dependency between the clock tone and the ICC, we used a MATLAB®-simulated 32-GBd PM-16QAM Nyquist-shaped signal (raised cosine, roll-off 0.15) with 19-dB OSNR. DGD and SoP rotation was introduced by the transformation:

$$\begin{pmatrix} \tilde{E}'_x \\ \tilde{E}'_y \end{pmatrix} = \begin{pmatrix} e^{-j\omega\tau/2} & 0 \\ 0 & e^{j\omega\tau/2} \end{pmatrix} \begin{pmatrix} \cos\theta & -\sin\theta \\ \sin\theta & \cos\theta \end{pmatrix} \begin{pmatrix} \tilde{E}_x \\ \tilde{E}_y \end{pmatrix}, \tag{1}$$

where θ is a rotation angle, ω is the angular frequency, τ is the DGD, and top tilde represents the frequency-domain. The signal was interpolated to emulate a receiver clock error, $\varepsilon_{\text{clk}} = 20$ ppm. Figs. 1(a-f) show the clock tone strength when the SoP of the received signal $[E'_x\ E'_y]^T$ is transformed by the Jones matrix:

$$\mathbf{J} = \begin{pmatrix} \cos\psi \cdot e^{-j\chi} & -\sin\psi \cdot e^{-j\chi} \\ \sin\psi \cdot e^{j\chi} & \cos\psi \cdot e^{j\chi} \end{pmatrix}, \tag{2}$$

where ψ and χ are the azimuth and ellipticity angles. The clock tone strength is computed by applying the modified Gardner phase detector [8] to a $2N$-sample sequence (2x oversampling), producing N (time varying) timing error estimates, ε_n; and then computing the discrete-time Fourier transform (DTFT) at the ε_{clk} frequency:

$$F_{\text{clk}} = \sum_{n=1}^{N} \varepsilon_n \cdot e^{-j2\pi n \varepsilon_{\text{clk}}}. \tag{3}$$

The first row (Figs. 1(a-c)) shows F_{clk} for selected θ when no DGD is applied ($\tau = 0$), while the second row (Figs. 1(d-f)) depicts the same signal with half-the-symbol-time DGD ($\tau = 0.5T$). The corresponding surfaces (a-d, b-e, c-f) show similar patterns; however, the clock tone is lost only when DGD $\approx 0.5T$. Note that, for $\theta \neq 0$, the surfaces provide

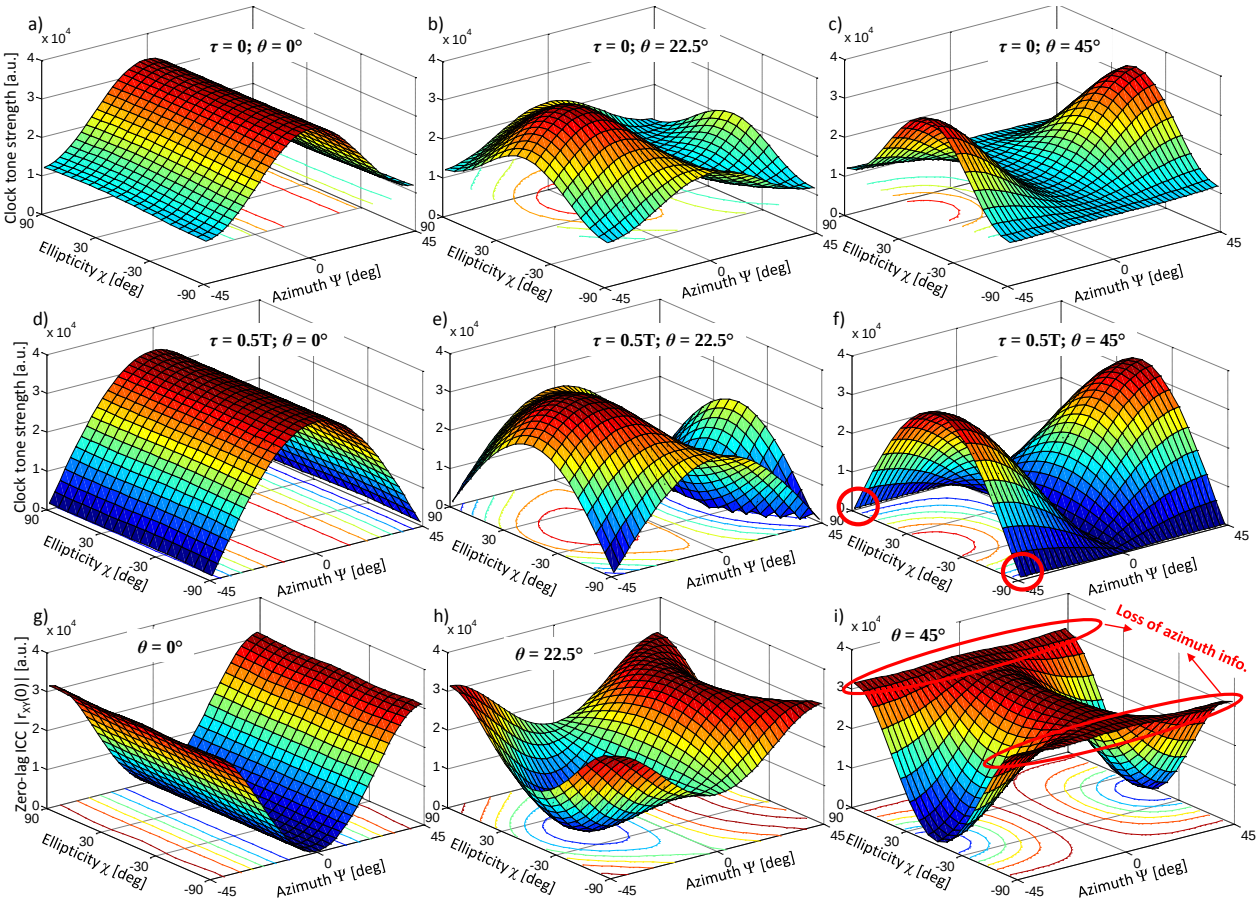

Fig. 1: Clock tone strength (a-c) without and (d-f) with $0.5T$ DGD; (g-i) corresponding X/Y-pol ICC.

complete information on the SoP. The third row (Figs. 1(g-i)) shows the corresponding absolute value of (unnormalized) ICC between the orthogonal polarizations, X/Y-pol, at zero lag:

$$|r_{XY}(0)| = \left| \frac{1}{N} \sum_{n=1}^{N} (|E'_{X_n}| - \overline{|E'_X|})(|E'_{Y_n}| - \overline{|E'_Y|}) \right|, \tag{4}$$

where $\overline{\{.\}}$ is the mean value. Unlike the clock tone, the ICC surfaces are not affected by τ, and therefore, are represented here by a single set of figures. Evidently, ICC carries all the SoP information, so that its minimization allows recovery of the clock tone. The mean values $\overline{|E'_{X/Y}|}$ in (4) vary little with the SoP, and can be considered constant. Thus, $|r_{XY}(0)|$ is simply the first term of $|\Re\{\text{IDFT}(\text{FFT}(|E''_X|)\text{FFT}^*(|E''_Y|))\}|$, where $|E''_{X/Y}| = |E'_{X/Y}| - \overline{|E'_{X/Y}|}$, and $\Re\{.\}$ represents the real part. Note that the two real-valued FFTs inside the parentheses can be implemented as a single complex FFT [7]. Further, for the first term, the outer IDFT is nothing but the mean value of $(\text{FFT}(|E''_X|)\text{FFT}^*(|E''_Y|))$.

Additional observation is that if the azimuth ψ is properly aligned, the clock tone is lost only when the signal is nearly circularly polarized; that is, $\chi \approx \pm 90°$ (as show red circles in Fig. 1(f)). Thus, a simple de-rotation, given by (2) when $\chi = 0$, should be able to recover it in most practical cases. Conversely, a fully circular SoP at $\theta = 45°$ results in loss of azimuth information (see Fig. 1(i)). This particular situation, though, can be resolved in many practical ways.

3. Experimental Validation

The experimental setup is depicted in Fig. 2. At the transmit-side, a 92-GSa/s arbitrary waveform generator (AWG, 32-GHz bandwidth, 8-bit resolution) generates four RF signals, corresponding to the in-phase (I) and quadrature (Q) components of X/Y-pol tributaries from pre-programed digital samples of a 32 GBd PM-16QAM Nyquist signal (raised cosine, roll-off 0.15). The RF outputs drive a 35-GHz InP PM-IQ modulator (PM-IQM) that modulates a 100-kHz linewidth external cavity laser (ECL). The DGD is applied by a polarization-maintaining programmable optical filter (POF), after aligning the signal SoP to the POF axes by a polarization controller. Amplified spontaneous emission noise, controlled by a variable optical attenuator (VOA), is coupled onto the signal to yield 20-dB OSNR, corresponding to bit error rate (BER) $\approx 1.8 \times 10^{-2}$. At the receive-side, X/Y-pol components are mixed at $\sim 45°$ by additional polarization

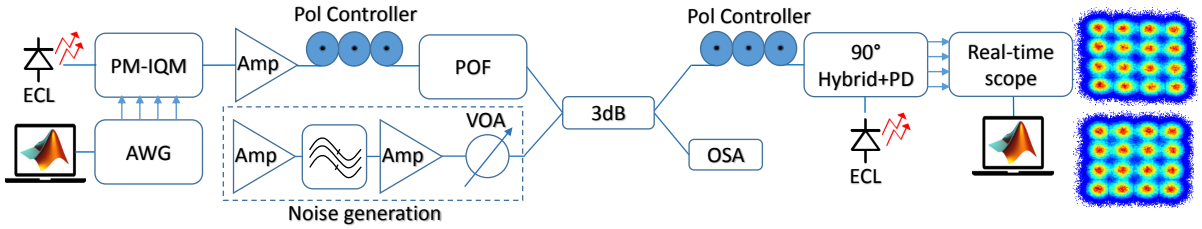

Fig. 2: Experimental setup.

controller, and detected by an integrated 25-GHz polarization diversity coherent receiver (100-kHz linewidth ECL LO). An 80-GSa/s real-time oscilloscope (33-GHz bandwidth, 8-bit resolution) samples and stores the four signal tributaries for offline post-processing.

Figs. 3(a-c) show the obtained results for 10, 20 and 40 ppm clock errors, respectively. We extracted the clock tone by applying the modified Gardner phase detector [8], followed by FFT, whose magnitude is plotted in the figures in a logarithmic scale. For each signal, 40 discrete rotation angles were applied (in the digital-domain) in the range of $\pm 45^{\circ}$, to select the one that resulted in the lowest ICC. The respective ICC profiles for all tested angles are shown in Figs. 3(d-f). In all cases, appropriate SoP rotation allowed to successfully recover the clock tone.

In real systems, with signal SoP changing over time, our method can be implemented using, e.g., a gradient descent algorithm, as in [6], or a hardware-efficient feedforward algorithm, similar to [9]. Associated challenges, such as tracking speed and SoP cycle slips exceed the scope of this work and should be further addressed.

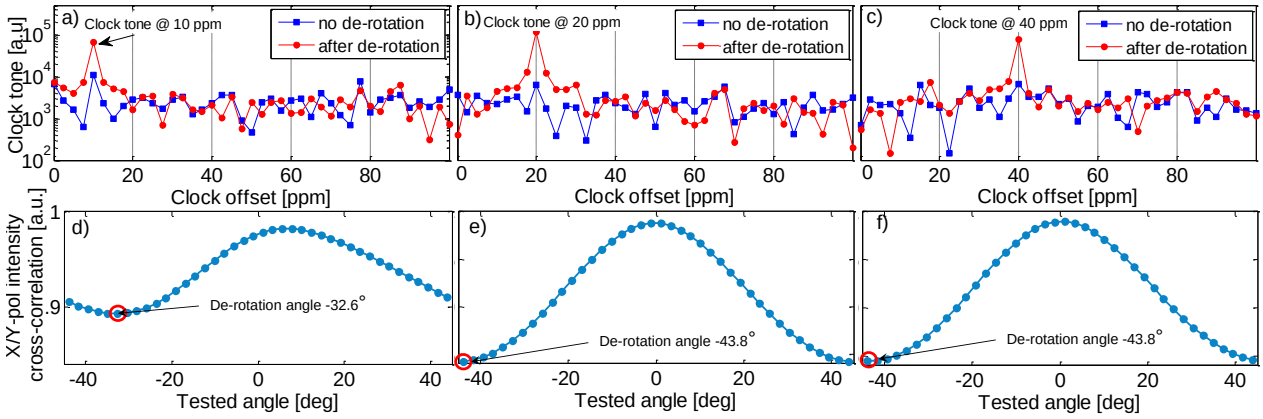

Fig. 3: Experimental results: (a-c) FFT magnitude (log. scale) of the modified Gardner phase detector output for 10, 20, and 40 ppm clock offset signals; (d-f) corresponding ICC values for SoP rotation between -45° and 45°.

4. Conclusion

We proposed and experimentally validated a clock tone recovery method in coherent optical systems through digital-domain SoP rotation. The method is based on minimizing the inter-polarization intensity correlation, which can be efficiently implemented via the FFT algorithm.

Acknowledgements

This work was supported by the Australian Research Council (FL130100041, CE110001018).

References

[1] W. C. Ng et al., "Enhancing clock tone via polarization pre-rotation: A low-complexity, extended Kalman filter-based approach," in "OFC/NFOEC," (2015). Th2A.19.
[2] N. Stojanović et al., "A circuit enabling clock extraction in coherent receivers," in "ECOC," (2012). P3.08.
[3] B. Szafraniec et al., "'polarization demultiplexing in Stokes space," Opt. Express **18**, 17,928–17,939 (2010).
[4] N. J. Muga and A. N. Pinto, "Adaptive 3-D Stokes space-based polarization demultiplexing algorithm," J. Lightwave Technol. **32**, 3290–3298 (2014).
[5] R. Schmogrow et al., "Blind polarization demultiplexing with low computational complexity"," IEEE Photon. Technol. Lett. **25**, 1230–1233 (2013).
[6] H. Sun and K. Wu, "A novel dispersion and PMD tolerant clock phase detector for coherent transmission systems," in "OFC/NFOEC," (Optical Society of America, 2011). OMJ.4.
[7] E. Chu and A. George, *Inside the FFT black box: serial and parallel fast Fourier transform algorithms* (CRC Press, 1999). Ch. 14.
[8] N. Stojanović et al., "Modified Gardner phase detector for Nyquist coherent optical transmission systems," in "OFC/NFOEC," (2013). JTh2A.50.
[9] T. Pfau et al., "Hardware-efficient coherent digital receiver concept with feedforward carrier recovery for M-QAM constellations," J. Lightwave Technol. **27**, 989–999 (2009).